WEP Warwick Evans Publishing

Transactions on Engineering and Technology Research
ISSN: 2960-1797, eISSN: 2960-2246 | Volume 1
AMMEE 2023

Development of a Vibration-based Experimental Platform for Diagnosing Gear Pitting Failure in Reducers

Juanjuan Li [1, 2, a], Guofang Wang [1, 2, b], Sen Jia [1, 2, c], Yun Wang [1, 2, d] and Yannan Liu [1, 2, e]

[1] Henan Special Equipment Inspection Technology Research Institute, No. 10, Baifo South Road, Zhengdong New Area, Zhengzhou, Henan, China

[2] National Center for Quality Inspection and Testing of Overhead, Gantry Cranes and Light Hoists (Henan), Zhengzhou, Henan, China

[a]cuci99@163.com, [b]shape19@163.com, [c]469136326@qq.com, [d]yuner0924@163.com, [e]tjlyn6@163.com

Abstract. Gear pitting failure in the reducer has a significant impact on the normal operation and transmission efficiency of the equipment. In this paper, a vibration-based experimental platform for diagnosing gear pitting failure in reducers is developed. The platform aims to simulate gear pitting failure conditions and analyze vibration signal characteristics. Through the validation of experimental results, this paper demonstrates that analyzing vibration parameters such as clearance, impulse, peak value, and vibration intensity, combined with the multiple relationship between fault frequency in vibration spectrum and gear meshing frequency, can accurately determine the type and location of gear failure in the reducer. Furthermore, the experimental platform can simulate gear vibration under different speeds and loads, providing a foundation for accurate diagnosis and identification of gear failures. The developed experimental platform has significant practical value and can provide technical support for the prevention and maintenance of gear failures in reducers.

Keywords: Gear pitting, vibration detection, characteristic signal, test bench.

1. Introduction

Gear reducer is an important mechanical transmission device widely used in various fields[1-2]. Gears are the most susceptible component to failures in gear reducers, with approximately 60% of failures being caused by gear pitting. Pitting failure not only leads to metal spalling on the gear surface but also causes tooth breakage, impact, noise, and reduces transmission efficiency[3]. Therefore, the detection of pitting failure in gears is of great significance for the development of gear fault diagnosis technology.

Many scholars have conducted in-depth research on the causes and subsequent effects of gear pitting and have proposed various diagnosis methods[4-6]. Among them, accurately diagnosing and preventing gear failure through the identification of the earliest vibration signal characteristics of gears is an important approach[7-9]. In order to study the effects of early-stage gear pitting failure on vibration signals, in this paper a vibration-based experimental rig for gear pitting fault diagnosis in gear reducers was developed. This experimental equipment can simulate different damage modes of gear reducers and simulate gear fault characteristics under different speeds and load torques. Which contribute to the foundation for gear fault recognition in gear reducers and the establishment of a gear fault database.

2. Composition of test bench

The test bench is shown in Figure 1, which is composed of six major systems, namely 1) Support system, 2) Power system, 3) Acceleration deceleration system, 4) Connection system, 5) Load system, 6) Control system, 7) Sensing system, 8) Output and display system.

Figure 1. Speed reducer fault diagnosis test bench

2.1. Support system

The support system of the test stand is a 5500x3000mm cast iron platform with a thickness of 200mm, equipped with T-slots for convenient connection of equipment.

2.2. Power system

The rated power of the power motor is 37kW, and it can achieve any speed between 0 and 1441r/min under the control of the frequency converter. During the test, the speed can be adjusted to the desired value using a manual knob. The motor can also change direction (reverse) at lower speeds.

2.3. Acceleration deceleration system

The speed changing system consists of two ZQ500-40 gearboxes arranged in a mirrored layout. The speed increasing system is a normal gearbox, which refers to a brand new gearbox without any faults. The speed decreasing system is also a gearbox of the same model, with pre-set point erosion faults implanted.

2.4. Connection system

The connection system refers to the coupling between the drive device and the gearbox. Elastic couplings are used for all couplings on the test stand.

2.5. Load system

The test bench uses a variable frequency speed-regulating torque motor as the load device, providing necessary reverse braking force for the entire experimental system. It can also feed back the generated electric energy to the power grid through a feedback device, saving 30-50% of energy.

2.6. Control system

The control system mainly consists of control circuits, frequency converters, PLCs, etc., which control the forward and reverse rotation of the motor, load force loading, and have functions such as overload and overcurrent protection.

2.7. Sensing system

The sensing system of the test stand includes the speed and torque sensor ZJ-500A between the drive motor and the gearbox, the torque and speed sensor ZJ-10000AE between the gearbox and the speed increasing system, and the speed and torque sensor ZJ-500A between the speed increasing system and the load motor. In addition, there are two temperature sensors.

2.8. Output and display system

The output and display system consists of two parts: the sensor direct output signal display system TS3000 torque, speed, and power acquisition instrument, and the display monitor connected to the computer for signal acquisition. The display monitor can display parameters and load conditions in different sections, and can also draw real-time curves. The output and display system are shown in Figure 2.

Figure 2. Output and display system

3. Gear pitting fault implantation

During the operation of gears, the position most susceptible to pitting is the tooth engagement area where the gears are subjected to alternating loads. The pitting occurs on the tooth surfaces near the pitch line and, with prolonged exposure to alternating stresses, it can develop into “spot to surface” damage. To simulate pitting faults in the gears, stamping technology was used to arrange simulated pitting marks near the gear tooth meshing surface. The diameter of each mark ranges from 0.1mm to 1mm, with 4-6 marks arranged on each meshing surface. The marks are evenly distributed across a gear using a “5-point gap, 1-point mark” pattern (gap between meshing surfaces). The placement locations are on the high-speed shaft gear tooth surface and the low-speed shaft gear tooth surface, while the intermediate shaft does not undergo treatment. The gear with the pitting marks and the positioning diagram are shown in Figure 3.

Figure 3. Gear pitting fault implantation diagram

4. Vibration signal acquisition

In typical cases, measurements need to be taken at two mutually orthogonal radial positions on each bearing cap or bearing seat. The sensor can be placed at any angle position on the bearing seat or machine bed. For horizontally mounted machines, measurements are usually taken in the vertical and horizontal directions. For vertical or inclined machines, the position that gives the maximum vibration measurement reading (usually along the direction of the flexible shaft) should be chosen as the orientation for sensor placement [10].

Measurements should be taken when the transmission system has reached its normal steady-state operating temperature and the machine is in the specified operating condition (such as rated speed, voltage, flow rate, pressure, and load). For machines with variable speed and load, measurements should be taken for all operating conditions that require the machine to operate for a long period.

In this experiment, based on the actual conditions of the gearbox, a dual-channel vibration sensor placement is shown in Figure 4. The sensors are arranged in the horizontal and vertical directions,

and on-site data acquisition of vibration data is performed. The horizontal and vertical directions of the bearing seat for the high-speed shaft of the gearbox during data acquisition can be seen in the arrows in Figure 4. Figure 5 shows the layout of measurement points. Vibration detection sensors are attached to the bearing seat in the form of magnetic holders and arranged orthogonally.

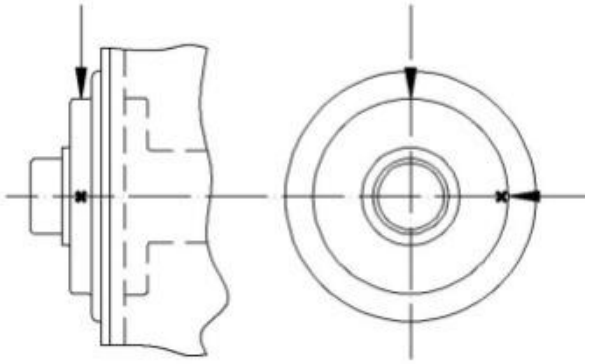

Figure 4. Schematic diagram of sensor measurement point arrangement

Figure 5. Field vibration data acquisition measurement point arrangement

The instrument used for acquire vibration signals is the PDES-E Equipment fault diagnosis system produced by INVT Technology Co., Ltd. The sensors used are magnetic holder type, and the collected signal is acceleration.

5. Vibration signal analysis

Layout of measuring points: see Fig. 4 and Fig. 5.

Detection condition: high speed shaft with input speed of 800r/min and zero load.

Transmission route map: ZQ500-40 reducer is composed of two-stage transmission [11], and the transmission route is shown in Figure 6.

$$\mathrm{I_{shaft}} - \frac{13}{86} - \mathrm{II_{shaft}} \begin{cases} \frac{86}{13}(\text{Speed:120 r/min}) \\ \frac{14}{85}(\text{Speed:19.76 r/min}) \end{cases}$$

Figure 6. Transmission road

When the input shaft is 800r/min, the rotation frequency of each shaft is shown in Table 1, and the gear meshing frequency of each transmission group is shown in Table 2.

Table 1. Speed rpm of each shaft of the reducer (800r/min)

axis number	speed（r/min）	rotating frequency（Hz）
I	800	13.3
II	120	2
III	20	0.33

Table 2. Gear meshing frequency of reducer (800r/min)

Drive group number	Gear-mesh Frequency
I-II	173
II-III	28

Vibration waveform-spectrum diagrams obtained from the collection of vibration data on the vertical end of the high-speed shaft of a normal gearbox are shown in Figure 7. Vibration waveform-spectrum diagrams obtained from the collection of vibration data on the high-speed shaft position of a faulty gearbox are shown in Figure 8.

Based on the comparison of the major vibration parameters in the time domain [12-14] at the same speed (800r/min), as shown in Table 3, each parameter value for the faulty gearbox is slightly higher than that of the normal gearbox. which indicate that the faulty gear gearbox has overall higher vibration compared to the normal gear gearbox. The significant differences in pulse index and kurtosis index suggest that there is a higher level of impact energy in the components at that measurement point.

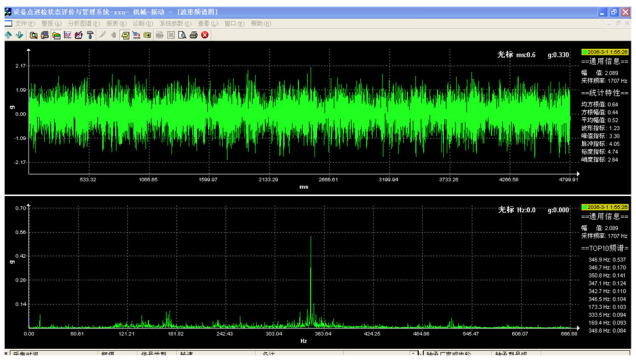

Figure 7. 800r/min fault-free gear waveform and spectrum

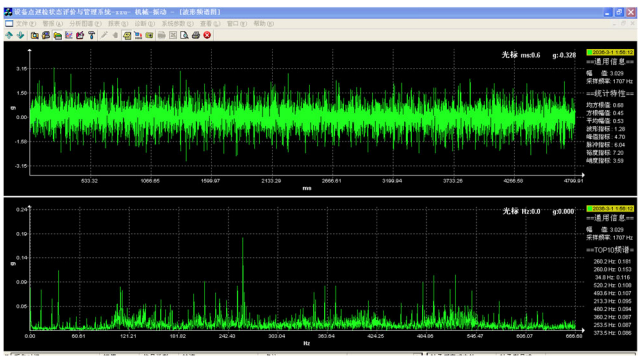

Figure 8. Faulty gear waveform and spectrum at 800r/min

Table 3. Comparison table of the main parameters of the time domain range

Vibration Parameter	Normal Gearbox Value	Faulty Gearbox Value	Difference
Root mean square value	0.64	0.68	0.04
Square root amplitude	0.44	0.45	0.01
Average amplitude	0.52	0.53	0.01
Waveform index	1.23	1.28	0.05
Peak index	3.30	4.70	1.40
Pulse index	4.05	6.04	1.99
clearance factor	4.74	7.20	2.46
kurtosis value	2.64	3.59	0.95

Based on the comparison of frequency and amplitude parameters in the frequency domain, as shown in Table 4, the measured values for the frequency spectrum and amplitude of the normal gearbox and faulty gearbox are given.

From Figure 8, it can be observed that the faulty gearbox contains more and more pronounced impact signals. By calculating, it is found that at the frequency of 520.2Hz, the fault frequency 173 is three times the meshing frequency, indicating the presence of defects on the gears of the I-II shaft [15]. Based on a preliminary analysis, it can be concluded that the fault is gear pitting on the high-speed shaft, which aligns with the expected location of the implanted fault.

In the same speed, the greatest variation in the main vibration parameters between the faulty gearbox and the normal gearbox is observed in the clearance index, with a relative change of 2.46. This indicates the presence of wear in the gearbox. The relative changes in the impulse index and peak value index are 1.99 and 1.40, respectively, indicating the presence of significant impact signals in the faulty gearbox. The relative change in the root mean square value (vibration intensity) is only 0.04, indicating that the wear condition in the early stage of the fault is minor and the vibration intensity is not significant.

Table 4. Frequency range frequency and amplitude

Serial Number	Normal Gearbox Value		Faulty Gearbox Value	
	Frequen(Hz)	amplitude	Frequency(Hz)	amplitude
1	346.9	0.573	260.2	0.181
2	346.7	0.170	260.0	0.153
3	350.8	0.141	34.8	0.116
4	347.1	0.124	520.2	0.108
5	342.7	0.110	493.6	0.107
6	346.5	0.104	213.3	0.095
7	177.3	0.103	480.2	0.094
8	333.5	0.094	360.2	0.087
9	169.4	0.093	253.5	0.087
10	248.8	0.084	373.5	0.086

6. Analysis and discussion

The maximum frequency of the faulty gearbox is 520.2Hz, and the sideband is significantly larger compared to the normal gearbox. This frequency is three times the meshing frequency of the gear, 173Hz, indicating the possibility of wear at the gear tooth surface contact area on the high-speed shaft

of the gearbox, possibly caused by pitting. The analysis confirms that the detection and analysis results of the faulty gearbox are consistent with the implanted fault type and position.

The experimental setup also includes other fault gears in the gearbox, such as gear tooth fracture and tooth surface adhesion caused by artificial faults. The gears in the gearbox can be replaced on-site, followed by vibration detection to establish a fault information database for gears with different characteristics, providing a practical basis for gear fault detection research. The experimental setup can also be used for long-term monitoring of gear faults, simulating field conditions to monitor and detect faulty gears over an extended period and obtain a characteristic database for gears with the same fault type but different degrees of damage.

7. Conclusion

This article developed a fault diagnosis test bench for detecting gear tooth surface pitting in gearboxes. The test bench not only simulates the failure detection of initial gear pitting, but also replicates the vibration signal characteristics of gears at different rotational speeds and load conditions. While the test bench is in operation, it can not only obtain the fault characteristics of pitted gears, but also the vibration characteristics of normal gear operation.

The fault vibration parameters, including margin indicators, impulse indicators, peak indicators, and vibration intensity, are significantly higher in the faulty gearbox compared to the normal gearbox. This indicates the presence of slight wear in the internal components of the faulty gearbox.

By comparing and analyzing the vibration spectrum graphs of the normal and faulty gearboxes, it can be inferred that the wear occurring at the tooth surface joint of the high-speed shaft in the faulty gearbox, which is in a 3 times frequency relationship with the meshing frequency, may be due to pitting. This is consistent with the implanted pitting fault during the experiment, as well as the location of the fault implantation.

Acknowledgments

Henan Provincial Market Supervision Administration Science and Technology Plan Project：《Research on Crane Assembly Inspection and Uncertainty Evaluation Based on Laser Tracking Technology》， Project No: 2020sj75.

References

[1] Zhou, J. Research progress on vibration and noise of gear reducers. Mechanical Transmission [J] .2014, 06, 163-170.

[2] Chaari, F., Baccar, W., Abbes, M. S., et al. Effect of spalling or tooth breakage on gear mesh stiffness and dynamic response of a one-stage spur gear transmission[J]. European Journal of Mechanics A/Solids, 2008.27(1), 691-705.

[3] Han, J., & Zhang, R. Mechanism and diagnostic technology of rotating machinery failures[M]. Beijing: Machinery Industry Press, 1997.

[4] Luo, Z., Gao, W., & Ding, J. Analysis of typical problems of open gear in crane lifting mechanism[J]. Hoisting and Conveying Machinery, 2017, 07, 64-67.

[5] Cheng, J., Wang, S., & Wu, T. Simulation of morphological characteristics of gear pitting based on extended finite element method[J]. Journal of Mechanical Engineering, 2016, 05, 99-105.

[6] Zhao, J. New explanation of the cause of involute gear pitting[J]. Mechanical Design, 2002, 07, 38-42.

[7] Cheng, J., Wang, L., & Xiong, Y. An improved cuckoo search algorithm and its application in vibration fault diagnosis for a hydroelectric generating unit[J]. Engineering Optimization, 2018, 1593-1608.

[8] Hao, W., Wang, H., & Dong, X. Research on gear fault feature extraction method based on full vector arrangement entropy[J]. Journal of Vibration and Shock, 2016, 11, 224-228.

[9] Huang, Y., & Huang, C. Optimization-based support vector classifier for vibration fault diagnosis of steam turbine-generator sets[J]. Procedia Engineering, 2012, 1816-1821.

[10] GB/T 6075.3-2001. Measurement and evaluation of vibration on non-rotating parts of machines. Part 3: Industrial machines with rated power greater than 15 kW and rated speeds between 120 r/min and 15000 r/min in field measurement.

[11] Deng, X. Application of vibration diagnostic technology in state detection and diagnosis of CNC machine tools[J]. Dalian Jiaotong University, 2019, 12.

[12] Fan, J., Xiao, B., & Gao, S. A real-time online method for diagnosing rotational machinery vibration faults[J]. Journal of Power Engineering, 2018, 38(02), 121-126.

[13] Ren, X., Shao, W., & Ma, W. Experimental study on the influence of lubricating oil additives on the vibration of rolling mill reducers. Vibration[J]. Testing and Failure Analysis, 2008, 9, 92-96.

[14] Wu, D. Design and implementation of gear box fault diagnosis system based on vibration signals[J]. Chongqing University, China. 2021.

[15] He, F., & Zhao, Q. Application of vibration diagnostic technology in gear box fault diagnosis[J]. Mining Engineering, 2014, 12(05), 32-34.